Structure
Article

Gating Mechanism of the Influenza A M2 Channel Revealed by 1D and 2D IR Spectroscopies

Joshua Manor,[1] Prabuddha Mukherjee,[2,3] Yu-Shan Lin,[2] Hadas Leonov,[1] James L. Skinner,[2,*] Martin T. Zanni,[2,*] and Isaiah T. Arkin[1,*]
[1]The Alexander Silberman Institute of Life Sciences, Department of Biological Chemistry, The Hebrew University of Jerusalem, Edmund J. Safra Campus, Givat-Ram, Jerusalem 91904, Israel
[2]Department of Chemistry, University of Wisconsin, Madison, WI 53706-1396, USA
[3]Present address: Department of Chemistry, University of Illinois at Urbana-Champaign, Urbana, IL 61801, USA
*Correspondence: skinner@chem.wisc.edu (J.L.S.), zanni@chem.wisc.edu (M.T.Z.), arkin@huji.ac.il (I.T.A.)
DOI 10.1016/j.str.2008.12.015

SUMMARY

The pH-controlled M2 protein from influenza A is a critical component of the virus and serves as a target for the aminoadamantane antiflu agents that block its H^+ channel activity. To better understand its H^+ gating mechanism, we investigated M2 in lipid bilayers with a new combination of IR spectroscopies and theory. Linear Fourier transform infrared (FTIR) spectroscopy was used to measure the precise orientation of the backbone carbonyl groups, and 2D infrared (IR) spectroscopy was used to identify channel-lining residues. At low pH (open state), our results match previously published solid-state NMR and X-ray structures remarkably well. However, at neutral pH when the channel is closed, our measurements indicate that a large conformational change occurs that is consistent with the transmembrane α-helices rotating by one amino acid register—a structural rearrangement not previously observed. The combination of simulations and isotope-labeled FTIR and 2D IR spectroscopies provides a noninvasive means of interrogating the structures of membrane proteins in general and ion channels in particular.

INTRODUCTION

The M2 protein has become a model system for understanding the H^+ gating mechanism of ion channels. M2 assembles into tetramers with a single α-helical transmembrane domain (Duff and Ashley, 1992; Holsinger and Lamb, 1991). Following viral internalization, at the low pH of the endocytic vesicles, histidine residues in the transmembrane domain of M2 are thought to protonate, thereby activating the protein (Pinto et al., 1992; Wang et al., 1995). Upon opening of M2, the viral lumen acidifies, which facilitates the release of the viral contents into the cell. This critical step in the infectious cycle of the virus renders M2 an important target for antiflu agents, such as amantadine. Finally, M2 is particularly amenable to structural analyses because a peptide that encompasses its transmembrane domain faithfully represents its tetramerization, H^+ channel, and drug-binding activity (Duff et al., 1992; Hu et al., 2006, 2007; Salom et al., 2000). As a result, it has been possible to structurally characterize the M2 peptide both by solid-state NMR (ss-NMR) (Nishimura et al., 2002) and X-ray crystallography (Stouffer et al., 2008). Therefore, the objective of our study was to characterize the structural transition that the M2 channel undergoes upon gating. Toward this end we have employed, and quantitatively assessed, a novel combination of 1D and 2D infrared (IR) spectroscopies, along with calculations, that is particularly suited for this challenging task: probing the structure and dynamics of membrane proteins in their native environments.

Our approach relies on a combination of linear dichroism measurements and 2D IR lineshape analysis, which are largely enabled by site-specific isotope labeling. Because isotope labels do not perturb protein structures, they can be placed in sterically confined locations, such as the channel lumen of membrane proteins (like we do herein) that may not tolerate electron spin resonance or fluorescence probes. Moreover, 2D IR spectroscopy holds especially important promise for following the structural kinetics of membrane proteins. Finally, all of these IR measurements are conducted in the protein's native environment: the lipid bilayer.

The M2 channel is an ideal system to assess the accuracy of our IR methodology because it is structurally well characterized (Nishimura et al., 2002; Stouffer et al., 2008). The utility of our approach is underscored by the results of this study. We discovered that the M2 channel undergoes a large structural rearrangement upon gating that has not been previously detected and which has implications for the drug and gating mechanism of this important drug target.

RESULTS AND DISCUSSION

Properties of Isotope Labels

The experimental approach that we have taken relies on linear dichroism measurements and 2D IR lineshape analyses. To gain site-specific structural information, we used 1-$^{13}C = {}^{18}O$ labels to spectroscopically isolate individual residues (Torres et al., 2000a, 2001). $^{13}C = {}^{18}O$ labeling creates a ~60 cm^{-1} shift in the amide I band, which largely decouples it from the remaining unlabeled amide I modes (Mukherjee et al., 2006a; Fang and Hochstrasser, 2005). As a result, it can be treated as an isolated vibrational mode whose frequency is influenced mostly by its immediate surroundings and that has a transition dipole independent of the rest of the peptide structure. The unlabeled amide

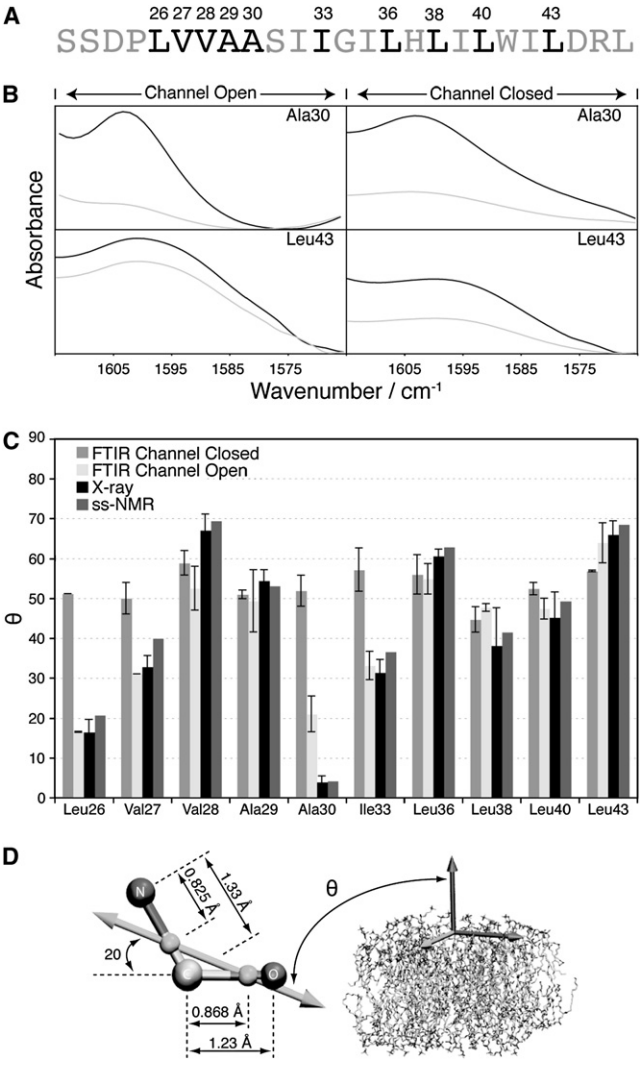

Figure 1. Results of the Linear FTIR Spectroscopy Measurements

(A) Sequence of the M2 transmembrane peptides used in all analyses. The black coloring signifies the 1-^{13}C = ^{18}O-labeled amino acids.

(B) Representative ATR-FTIR spectra of the M2 peptide in lipid bilayers focusing on the isotope-edited band of the amide I mode. The spectra were collected with parallel or perpendicular polarized light, black, and light gray curves, respectively. Spectra of all labels are shown in Figure S2.

(C) A comparison between the tilts of the transition dipole moments of the amide I mode derived from the FTIR studies at acidic (light gray) or neutral pH (gray), and those determined from the X-ray (black; Stouffer et al., 2008) and ss-NMR (dark gray; Nishimura et al., 2002) structures.

(D) Schematic diagram of the orientation of the transition dipole moment of the amide I mode relative to (i) the amide group's molecular frame according to Torii and Tasumi (1992) and to (ii) the bilayer normal, given by the angle θ.

I band that remains after isotope labeling contains significant structural information, and isotope editing can be used to help unravel its structural content. However, in what follows we focus on the labeled modes themselves.

Linear FTIR Dichroism Reveals Structural Differences between Low and High pH

The dichroisms that we have measured by attenuated total reflection Fourier transform infrared (ATR-FTIR) spectroscopy are of amide I vibrational modes of individual carbonyl groups in aligned bilayers. These data are then converted into the angles between the transition dipole moments of the labeled carbonyl groups and the bilayer normal. Because the orientation of the transition dipole moment of the amide I mode relative to the molecular frame is known (Torii and Tasumi, 1992), such dichroism measurements yield the angle between the bilayer normal and the carbonyl group (see Figure 1D). Thus, henceforth we refer to our measurements as yielding the angle between the bilayer normal and the C = O bond. The precise procedures for deriving the aforementioned angle is according to protocols that we have established in the past (Manor et al., 2005) and are outlined in Supplemental Data available online. Briefly, the process consists of (i) reconstituting the labeled channels in hydrated vesicles, (ii) removing bulk solvent while depositing the membranes on a solid support to create aligned bilayers, (iii) measuring the dichroism using ATR-FTIR spectroscopy, (iv) assessing the bilayer disorder by X-ray scattering (Figure S1) and, finally, (v) converting the measured dichroisms to the angles of the carbonyl groups with respect to the membrane normal. We followed this procedure for ten residues spread along the length of the peptide (as listed in Figure 1A) at acidic (pH 4) or neutral/basic conditions (pH 7 to 9) in which the channel is open or closed, respectively (Pinto et al., 1992).

To demonstrate how sensitive the dichroisms are to the carbonyl orientations in the bilayer, the FTIR spectra of Ala30 and Leu43 are shown in Figure 1B (FTIR spectra of all labeled peptides are shown in Figure S2). The dichroisms at acidic conditions of Ala30 and Leu43 are 18 ± 8 and 1.4 ± 0.2, respectively. These measurements in turn correspond to dramatically different angles of the carbonyl groups of Ala 30 and Leu43 from the membrane normal of 21° ± 4° and 64° ± 5°, respectively.

The accuracy of our method is assessed by a comparison of the angles we determined using IR spectroscopy at acidic conditions to the ss-NMR (Nishimura et al., 2002) and X-ray structures (Stouffer et al., 2008). A remarkably good agreement with the previously determined structures is observed (compare the light gray with the black and dark gray bars in Figure 1C). The average discrepancy is 6° ± 6° and 7.6° ± 5° between the IR-derived angles and the X-ray and ss-NMR structures, respectively. The angular differences between the ss-NMR and X-ray data are 3.2° ± 2°.

Angular data may be used to construct the backbone structures of proteins by an orientational refinement procedure (Nishimura et al., 2002). Rather than using a flexible peptide model and allowing the dihedral angles to vary for every residue, we have taken a conservative approach and fit our IR bond angles to a rigid helix. The angular refinement consisted of rotating and tilting the helix from the membrane normal and computing the angular deviation from our data, which is plotted in Figure 2 (top). The minimum deviation occurs for a helix tilted by 27° and rotated by 290°. Despite the fact that the peptide was treated as an ideal helix, this configuration is in close agreement with the structures previously determined by ss-NMR (Nishimura et al., 2002) and X-ray crystallography (Stouffer et al., 2008), with a backbone RMSD between individual helices of 2.4 Å and 2.5 Å, respectively. For comparison, the backbone RMSD between the ss-NMR and X-ray structures is 2.8 Å. Thus, we conclude that the dichroisms provide a quantitatively reliable way of characterizing the backbone structure of membrane proteins.

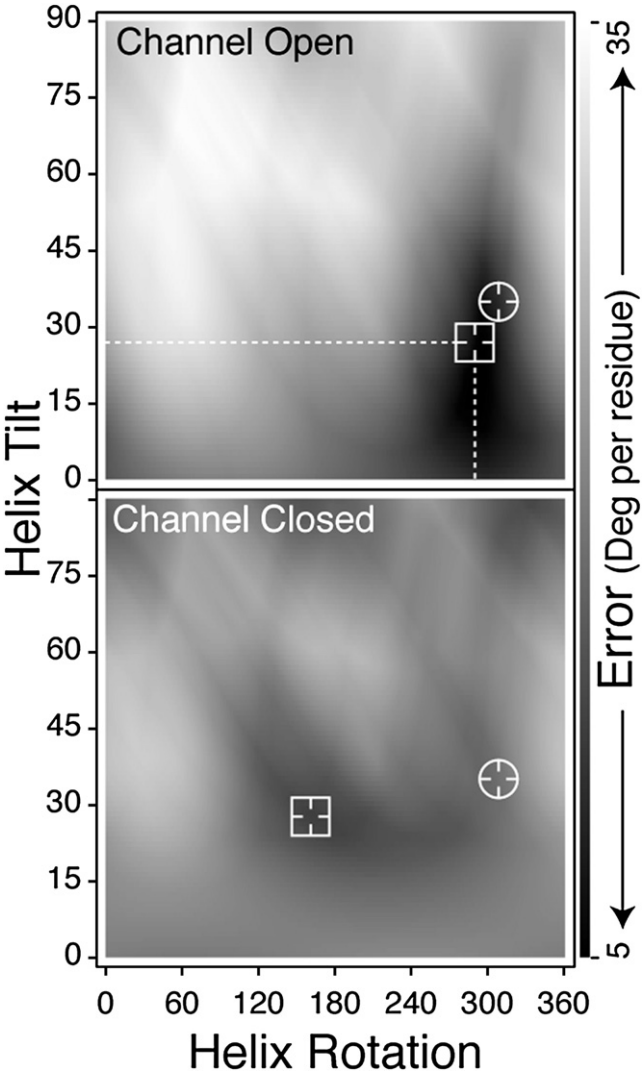

Figure 2. Rigid-Body Refinement of the M2 Protomer according to the FTIR-Derived Angles

Each point in the graph represents a particular combination of tilt and rotation angles for an ideal helix. The gray scale represents the difference per residue (in angles) that the structure has relative to the angles derived from the FTIR study (Figure 1C). The white squares represent the helix tilt and rotation combinations that resulted in the smallest deviation form the experimental results. The white circle represents the tilt and rotation of the helices of the X-ray structure (Stouffer et al., 2008).

2D IR Reveals a Shift in the Channel's Pore-Lining Residues

We next collected 2D IR spectra of the same ten isotopically labeled carbonyl groups using a photon echo pulse sequence at acidic conditions. An example of a 2D IR spectrum for Ile33 is shown in Figure 3A (spectra of all labeled peptides are presented in Figure S3). The isotope label appears near 1590 cm^{-1} and is highlighted with a gray arrow in the magnitude spectra. We found in our previous work on the CD3ζ transmembrane peptide (Mukherjee et al., 2004, 2006a, 2006b) that the diagonal linewidths of membrane peptides reflect the disorder of their surrounding electrostatic environments and that one of the biggest factors is the carbonyl's contact with water, which changes the amount of inhomogeneous broadening (Fang and Hochstrasser, 2005; Fang et al., 2006; Zheng et al., 2007). Because M2 is a transmembrane bundle like CD3ζ, we expect that the diagonal linewidths will scale with the depth of the residue in the bilayer as the lipid tails only weakly interact with the peptide backbone. To extract the linewidths from the data, we followed the same procedure as for CD3ζ (Mukherjee et al., 2004, 2006a, 2006b) and fit the spectra to a sum of 2D lineshapes. The resulting homogeneous and inhomogeneous linewidths are given in Tables S1 and S2, as are population relaxation times, which were measured by collecting a series of 2D IR spectra as a function of the waiting time in the pulse sequence. Each peptide was independently measured and fit at least three times to ensure the reproducibility of our results and to estimate error bars (a total of 60 2D IR spectra were collected for this study). Details of the fitting procedure, fits to the data, and error estimates are presented in Supplemental Data.

The diagonal linewidths of each amide carbonyl are plotted in Figure 3B (see Figure 3A, top, for a representative linewidth measurement of Ile33). As expected from our studies on CD3ζ (Mukherjee et al., 2004, 2006a, 2006b), residues at the ends of the peptide near the membrane interface have the largest diagonal linewidths, whereas residues in the middle of the membrane have the narrowest linewidth, because the diagonal linewidths scale with the environmental electrostatics. In addition, we also find that the 2D IR linewidths are sensitive to water inside the channel pore. This effect is best observed at the N-terminal end of the peptide, where we were able to label five consecutive residues (Leu26 to Ala30) so that the linewidth of every amino acid was measured for 1.5 turns of the helices. The data in this range reveal an oscillatory trend in linewidths, and comparison with the X-ray structure (Stouffer et al., 2008) shows that the linewidths correlate very well to the location of the residue in the helix. This correlation is highlighted in Figure 3B, where the positions of residues relative to the channel lumen are shown. For example, the inhomogeneous linewidth of Ala30 located at the channel lumen is higher than the linewidth of Ala29 located in the protein-protein interface. Leu36 has the narrowest linewidth because it is both in the middle of the bilayer and on the outside of the bundle.

Molecular Dynamics Simulation of the Pore-Lining Residues Reveals a Similar Picture

To further substantiate our observation that the linewidths indicate which residues line the channel pore, we have simulated 2D IR linewidths from a molecular dynamics trajectory. To accomplish this simulation, we equilibrated the X-ray crystal structure of M2 (Stouffer et al., 2008), assuming that three of the His37 residues are protonated (Hu et al., 2006; Chen et al., 2007), in a hydrated lipid bilayer, followed by a 1 ns molecular dynamics production trajectory. In calculating the spectra, because the amide I modes are isotopically labeled to create a substantial diagonal frequency shift (~60 cm^{-1}; Torres et al., 2000a, 2001), it is not necessary to include explicit coupling to the unlabeled C = O modes. We calculated the projection of the electric field onto the M2 amide groups at

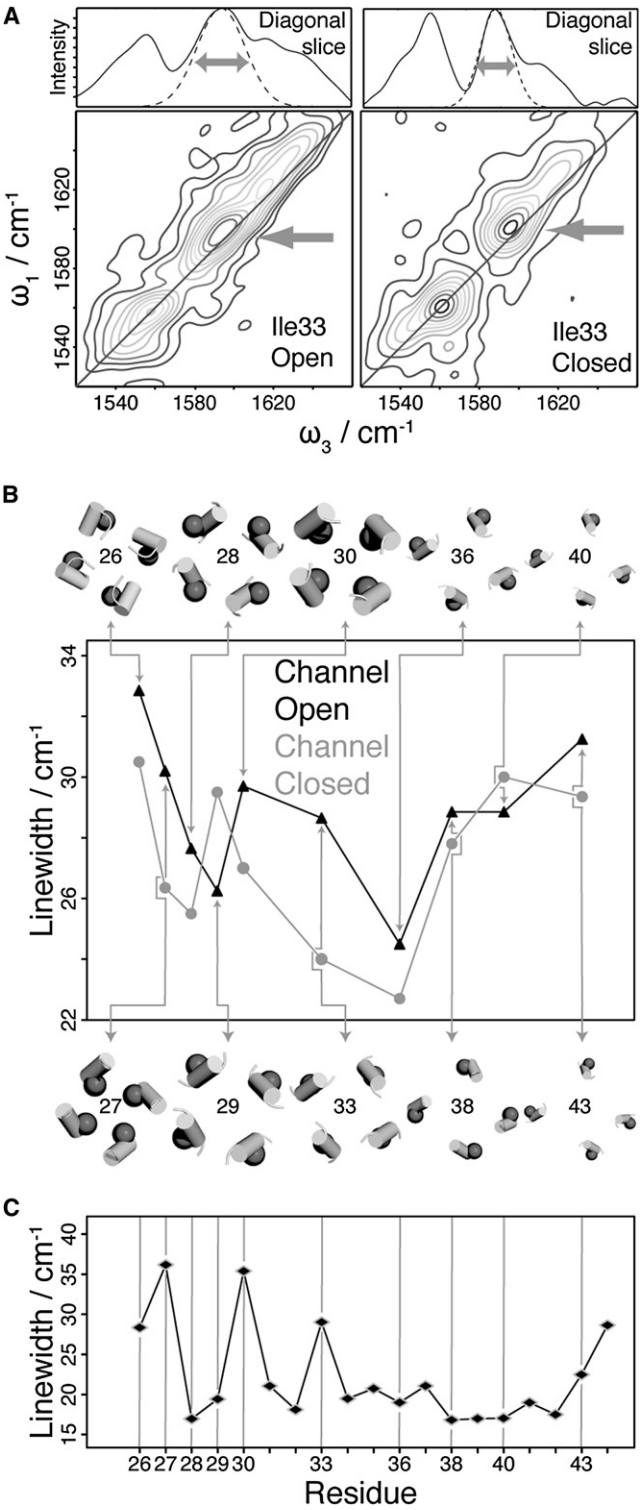

Figure 3. Results of the 2D IR Spectroscopy Measurements and the Molecular Dynamics Simulations

(A) 2D IR spectra of Ile33 at acidic (left) and neutral (right) conditions. The isotope-labeled peak appears at 1690 cm^{-1} and is highlighted with an arrow. (Top) Slices along the diagonals of the 2D IR spectra are shown along with a slice through the fit to the labeled peak that highlights the measured diagonal width (full fitting procedures and data sets are given in Supplemental Data).

(B) Diagonal linewidths extracted from the 2D IR spectra of the ten measured residues at acidic (black triangles) and basic (gray circles) conditions. The positions in the helix bundle of the labeled group (carbonyl oxygen in dark gray), which correlate with the 2D IR data, were taken from the X-ray structure (Stouffer et al., 2008). The data are presented in a numerical format in Tables S1 and S2, which includes error bars.

(C) Calculated diagonal linewidths from molecular dynamics simulations of the M2 peptide in lipid bilayers. Note the increased linewidths at residues 27, 30, and 33, which are the residues that line the channel pore. Error bars in the calculations are given in Table S3.

each step in the simulation. The electric fields were then converted into frequencies using a correlation map to give a frequency trajectory, which is used to calculate the 2D IR spectra (Lin et al., 2009). The details of this procedure are given in Supplemental Data. The simulated linewidths of the 2D IR magnitude spectra are shown in Figure 3C. Like the experiment, the calculated linewidths are largest at the terminal ends and narrowest in the middle, which reflect the water content in the membrane. Furthermore, residues 27, 30, and 33 have broad linewidths, consistent with their presence in the pore of the channel. Thus, while not in quantitative agreement, the simulations support the experimental observation that the linewidths reflect which residues line the channel pore. From the simulations and experiment, we conclude that the phase of the oscillatory trend is a measure of the rotational angle of the helices with regard to the channel pore.

Having established the information content of our 1D and 2D IR approach using a well-characterized protein structure, we turned to studying the structural changes associated with channel gating by performing the same experiments at neutral/basic conditions when the channel is in its closed state (Pinto et al., 1992). We find that many of the residues change their linewidths, as shown for Ile33 in Figure 3A (all of the 2D IR data and fits are given in Figures S3–S5). At neutral conditions, the largest linewidths are still observed at the ends of the helices, and the narrowest in the middle, indicating that the structure of the closed channel lies at about the same depth as when it is open. However, the phase of the oscillation between residues Leu26 and Ala30 is now shifted by about one residue (see Figure 4, top panel). For instance, Ala30, which had a very large linewidth because it was located inside the pore in the open state, now has a linewidth that is comparable to the narrow linewidths of dehydrated residues on the outside of the bundle. In contrast, Ala29 shows the opposite trend, indicating that it is exposed to a much stronger electrostatic environment in the closed state in comparison to the open state, strongly suggesting that it has become hydrated. In comparison, the C-terminal end shows little difference in linewidths between the closed and open states. This may be due to the fact that the protein forms a cone-shaped structure in which the N terminus is well packed and the C-terminal segment forms fewer protein-protein contacts (Stouffer et al., 2008). Thus the accessibility to water of individual residues at the C terminus is already high and therefore does not depend on their rotational position. Taken together, the most straightforward interpretation of the 2D IR linewidth changes is that the helices rotate by one amino acid register upon channel activation, such that the channel is lined by different sets of residues in the open and closed states.

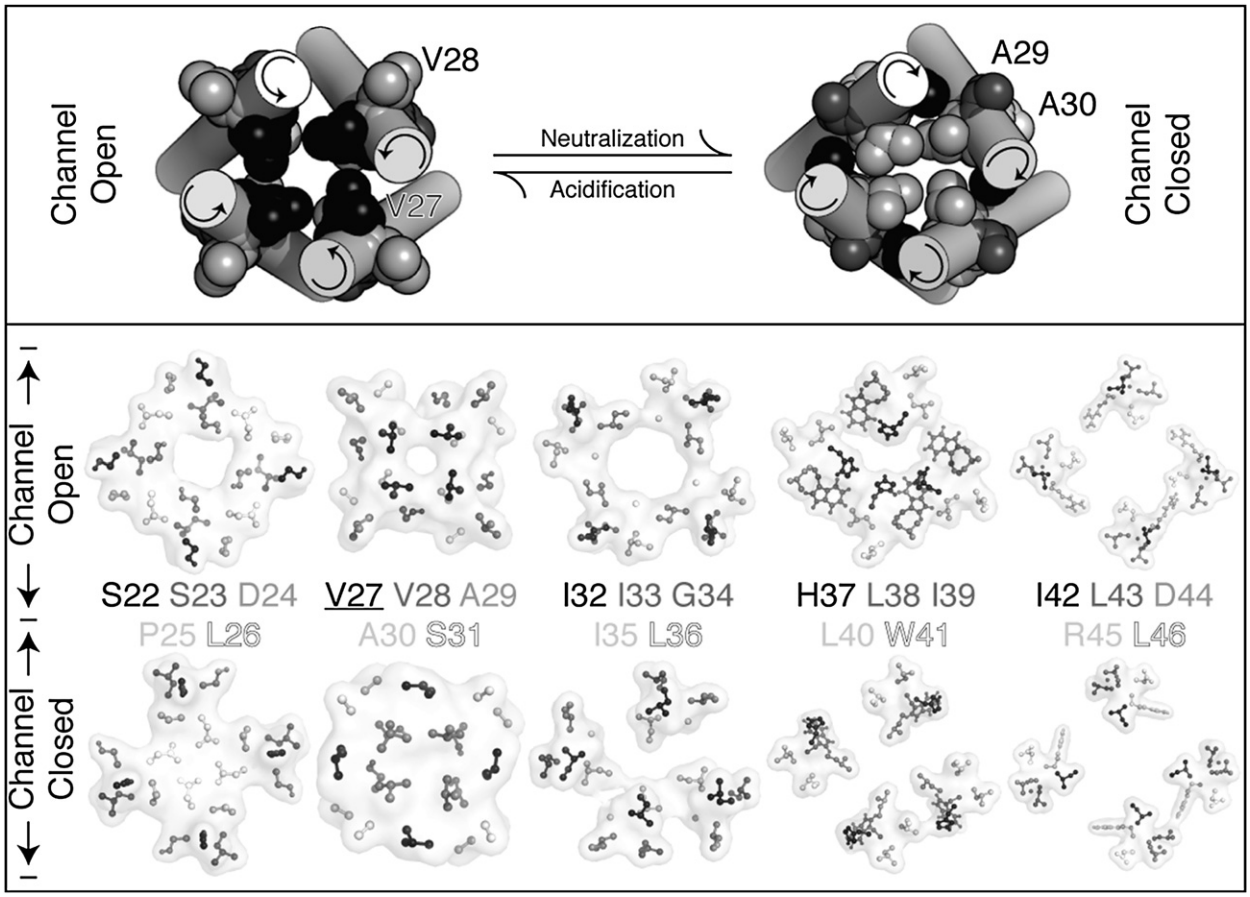

Figure 4. Visualization of the Proposed Gating Mechanism

(Top) The location of residues Val27–Ala30 in our models of the closed and open conformations of the M2 channel. Note the different rotational location of the residues that is consistent with the 2D IR data shown in Figure 3.

(Bottom) Slices through the M2 tetrameric complexes constructed according to the FTIR derived angles at the two pH conditions. The location of the labeled carbonyl group (underlined residues), are shown in CPK representation.

Large Angular Changes Observed between the Two pH Conditions Imply a Large Conformational Change, Simulated by Rigid-Body Refinement

To gain a more detailed insight into this structural change, we turned back to our 1D dichroism measurements, which we repeated at neutral conditions. The extracted angles between the labeled C = O groups and the bilayer normal are shown in Figure 1C (gray bars). We find substantial changes in the carbonyl angles from acidic to neutral conditions, especially at residues Leu26, Ala30, and Ala33, where the angles change by >30°, indicating large structural changes in the helices. It is important to realize that an observed change in the angle between a carbonyl bond and the bilayer normal mandates a structural change of the protein. However, a lack of a change in the carbonyl bond angle does not mean that a structural change did not occur, because a single carbonyl group's projection on the membrane normal does not restrain a structure unambiguously. We also note that it is merely a geometrical coincidence that the angles measured for the closed channel do not exhibit the extent of variation that was observed for the open channel.

To quantify the structural change that accompanies gating, we once again employed rigid-body refinement, rotating and tilting the helix to make a new refinement map based on the angles collected at neutral conditions. The new map, shown in Figure 2 (bottom) has a minimum at the same tilt angle (28°), but with a rotational angle that is 129° different from the configuration obtained at acidic conditions. Thus, according to both the 1D and 2D IR data sets, the helices conserve their tilt but undergo a large rotation, suggesting that the channel pore is lined by a number of different residues at acidic conditions compared with neutral state. Specifically, if under acidic conditions residue number *i* lines the pore, at neutral conditions, residue *i* + 1 faces the pore. Finally, we note that the discrepancy between the experimental results and the refinement model of the closed channel is higher than that of the open channel. In Figure S6, we plot the errors for the individual residues and find that the overall error is not larger because of a single residue, but is generally larger for all of the residues. This might indicate that the approximation of an ideal helix is a better assumption in the open state than in the closed state. Regardless, this structure is not in agreement with the ss-NMR

or X-ray-derived M2 bundles, because the helices are rotated by 100° to 130°.

Fully Constructed Model Reveals the Properties of the Open and Closed States, Supporting the Rotation by One Amino Acid Register

To better understand the pore structure and the gating movement that we observed, we constructed the tetrameric complex from the optimized helices at the two pH conditions. Our IR data do not currently yield distance constraints between the helices, which are necessary to reliably construct the ion channel from four individual helices. We therefore constructed the channel complex using the interhelical distances measured in the X-ray structure (Stouffer et al., 2008). Thus, the helices are constrained at the tilt and rotations predicted by our data, translated to proper relative distances, and the side-chains were allowed to relax. Slices through the two complexes, which include a surface representation looking at the channel from the N terminus, are shown in Figure 4. At neutral conditions, we find that the channel is closed, and at acidic conditions the channel is open, consistent with physiological results (Pinto et al., 1992). Thus, a gating mechanism that is coupled to rotational motion of the helices can explain our results.

The points of contact that seemingly close the channel in neutral conditions are Asp24 and Val28. Asp24 is one of the most conserved residues in the channel, and together with His37 they are the only ionizable residues in the membrane vicinity. Therefore it is tempting to speculate that both His37 and Asp24 undergo a change in protonation state upon channel activation. Under acidic conditions, His37 would be charged and water accessible, whereas Asp24 would be neutral and potentially water inaccessible. Under neutral conditions the reverse will transpire, leading to exposure of Asp24 and sequestration of His37. Interestingly, that is exactly what we observe in our model shown in Figure 4. Further experimentation is needed to substantiate this hypothesis.

Other membrane proteins undergo rotational motion upon gating. For example, the pore-lining helices of the acetylcholine receptor are thought to rotate upon binding acetylcholine, although the extent of rotation is still under debate (Law et al., 2005; Miyazawa et al., 2003; Sansom, 1995). Similarly, both the large and small conductance mechanosensitive channels from *E. coli* contain helices that are thought to undergo significant rotation upon activation (Bartlett et al., 2006; Edwards et al., 2005). Finally, thiol-disulfide equilibria mapping (Stouffer et al., 2008) as well as ss-NMR experiments (Bauer et al., 1999; Tian et al., 2003; Li et al., 2007) suggest that the M2 sequence is particularly tuned toward reduced stability that may accompany large motions.

Based on these findings, we conclude the following: (i) Our low pH results, both in terms of hydration and orientational data, are highly consistent with the previously available structures determined by either ss-NMR (Nishimura et al., 2002) or X-ray crystallography (Stouffer et al., 2008). (ii) Both our 1D and 2D IR data sets consistently point to a large structural reorganization between acidic and neutral pH, leading to a structure that is significantly different from published ss-NMR (Nishimura et al., 2002) and X-ray (Stouffer et al., 2008) structures.

An important strength of our approach is that we are able to study membrane proteins in the natural environment of a lipid bilayer and, because of the high sensitivity of IR spectroscopy, at near-physiological protein-to-lipid ratios (<1:20 by weight). As a result, we can ascertain the accuracy of structures obtained by X-ray crystallography or ss-NMR, which are performed in detergent micelles or at high protein-to-lipid ratios. The ability to double-check structures in bilayers is important because detergents can alter the energetics and structures of the transmembrane helices, as was documented for human glycophorin A and EmrE (Fisher et al., 1999, 2003; Soskine et al., 2006).

In this study, we find that the structures determined by ss-NMR (Nishimura et al., 2002) and X-ray crystallography (Stouffer et al., 2008) are structurally accurate as compared with our structure, but only if those experiments examined the channel in its open state, not the closed state. High protein-to-lipid ratios, or detergents, as discussed previously, could cause this discrepancy, but it could also be caused by a difference in pH, as the pH is responsible for gating in M2. pH can be difficult to maintain in samples with reduced hydration, like that used in ss-NMR, and unknown in crystal structures, especially because heavy metals used in crystallization may act as acids. But now, with 1D and 2D IR spectroscopies, it is possible to provide an independent check on the structures of proteins using backbone hydration and conformation data. The ability to probe hydration levels in ion channels without structural perturbation is particularly appealing, especially because 2D IR lineshapes can be predicted from molecular dynamics simulations (Schmidt et al., 2004; Choi et al., 2005; la Cour Jansen et al., 2006; Zhuang et al., 2006), as we demonstrated here.

In summary, we have found that a pH change induces a large-scale conformational change in the channel structure. Though our results might be explained by a number of possible structural changes, the 2D IR linewidths suggest that the channel pore is lined by a different set of residues in the open and closed states. Moreover, this change is highly consistent with our angular constraints derived from linear FTIR spectroscopy. This change has implications for the binding of amantadine or other drugs to the channel, as a change in residues will change the size and hydrophobicity of the channel. During the course of these experiments, we have also demonstrated the utility of infrared spectroscopy to quantitatively and qualitatively assess the structure of a membrane peptide channel. These methodologies might find use on other ion channel systems or be applied in a time-resolved manner to study membrane protein dynamics.

EXPERIMENTAL PROCEDURES

Linear FTIR Spectra

The synthesis, labeling, purification, and lipid reconstitution of the peptides used in this work have been described elsewhere (Torres et al., 2000a, 2000b) and are specified in detail in Supplemental Data. Similarly, the ATR-FTIR spectroscopy and the X-ray scattering, bilayer mosaicity estimation were undertaken as described elsewhere (Manor et al., 2005; Torres et al., 2000b) and are specified in detail in Supplemental Data.

2D IR Spectra

The experimental procedure for collecting heterodyned 2D IR spectra is given in detail elsewhere (Fulmer et al., 2004) and described in Supplemental Data. To extract the 2D lineshape of the labeled amide I mode, we follow our previously established fitting procedure of using the Fourier transform of the third-order response in the limit of Bloch dynamics with a pure dephasing time of T_2^* and an inhomogeneous distribution of Δ_0 (Mukherjee et al., 2004).

pH Control

The pH control in our experiments was conducted as follows. In the ATR-FTIR work, HCl, NaOH, and PBS were used to bring the solution to a final pH of 4, 7, or 9, respectively. The pH was monitored throughout the entire process, including during the removal of the bulk solvent from the sample before measuring the FTIR spectra, and was found to change only marginally in all three preparations. The three different conditions had no visible effect on the FTIR spectra. HCl-treated preparation is addressed as low pH samples throughout this work, whereas PBS- or NaOH-treated preparations are addressed as neutral/basic pH samples. No differences in the results were obtained between preparations with PBS or NaOH. In the 2D IR work, the vesicles resided in excess water. For the closed-state measurements, the pH was checked by blotting a small amount on pH paper. For the open state, the sample was buffered to pH 5.

SUPPLEMENTAL DATA

Supplemental Data include Supplemental Experimental Procedures and References, six figures, and three tables and can be found with this article online at http://www.cell.com/structure/supplemental/S0969-2126(09)00033-1.

ACKNOWLEDGMENTS

We thank W.F. DeGrado for thoughtful discussions. This work was supported in part by grants from the National Institutes of Health (R21AI064797 to M.T.Z. and I.T.A.), the National Science Foundation (CHE-0832584 to J.L.S. and M.T.Z.), and the Israeli Science Foundation (784/01, 1249/05, and 1581/08 to I.T.A.). J.L.S. thanks the National Science Foundation (CHE-0750307) for support. I.T.A. is the Arthur Lejwa Professor of Structural Biochemistry at the Hebrew University of Jerusalem. Molecular figures were generated by PyMOL (DeLano Scientific, LLC, San Francisco).

Received: November 5, 2008
Revised: December 4, 2008
Accepted: December 7, 2008
Published: February 12, 2009

REFERENCES

Bartlett, J.L., Li, Y., and Blount, P. (2006). Mechanosensitive channel gating transitions resolved by functional changes upon pore modification. Biophys. J. *91*, 3684–3691.

Bauer, C.M., Pinto, L.H., Cross, T.A., and Lamb, R.A. (1999). The influenza virus M2 ion channel protein: probing the structure of the transmembrane domain in intact cells by using engineered disulfide cross-linking. Virology *254*, 196–209.

Chen, H., Wu, Y., and Voth, G.A. (2007). Proton transport behavior through the influenza A M2 channel: insights from molecular simulation. Biophys. J. *93*, 3470–3479.

Choi, J.H., Hahn, S., and Cho, M. (2005). Amide 1 IR, VCD, and 2D IR spectra of isotope-labeled alpha-helix in liquid water: numerical simulation studies. Int. J. Quantum Chem. *104*, 616–634.

Duff, K.C., and Ashley, R.H. (1992). The transmembrane domain of influenza A M2 protein forms amantadine-sensitive proton channels in planar lipid bilayers. Virology *190*, 485–489.

Duff, K.C., Kelly, S.M., Price, N.C., and Bradshaw, J.P. (1992). The secondary structure of influenza A M2 transmembrane domain. A circular dichroism study. FEBS Lett. *311*, 256–258.

Edwards, M.D., Li, Y., Kim, S., Miller, S., Bartlett, W., Black, S., Dennison, S., Iscla, I., Blount, P., Bowie, J.U., and Booth, I.R. (2005). Pivotal role of the glycine-rich TM3 helix in gating the MscS mechanosensitive channel. Nat. Struct. Mol. Biol. *12*, 113–119.

Fang, C., and Hochstrasser, R.M. (2005). Two-dimensional infrared spectra of the 13C=18O isotopomers of alanine residues in an alpha-helix. J. Phys. Chem. B *109*, 18652–18663.

Fang, C., Senes, A., Cristian, L., DeGrado, W.F., and Hochstrasser, R.M. (2006). Amide vibrations are delocalized across the hydrophobic interface of a transmembrane helix dimer. Proc. Natl. Acad. Sci. U.S.A. *103*, 16740–16745.

Fisher, L.E., Engelman, D.M., and Sturgis, J.N. (1999). Detergents modulate dimerization, but not helicity, of the glycophorin A transmembrane domain. J. Mol. Biol. *293*, 639–651.

Fisher, L.E., Engelman, D.M., and Sturgis, J.N. (2003). Effect of detergents on the association of the glycophorin a transmembrane helix. Biophys. J. *85*, 3097–3105.

Fulmer, E.C., Mukherjee, P., Krummel, A.T., and Zanni, M.T. (2004). A pulse sequence for directly measuring the anharmonicities of coupled vibrations: two-quantum two-dimensional infrared spectroscopy. J. Chem. Phys. *120*, 8067–8078.

Holsinger, L.J., and Lamb, R.A. (1991). Influenza virus M2 integral membrane protein is a homotetramer stabilized by formation of disulfide bonds. Virology *183*, 32–43.

Hu, J., Fu, R., Nishimura, K., Zhang, L., Zhou, H.X., Busath, D.D., Vijayvergiya, V., and Cross, T.A. (2006). Histidines, heart of the hydrogen ion channel from influenza A virus: toward an understanding of conductance and proton selectivity. Proc. Natl. Acad. Sci. U.S.A. *103*, 6865–6870.

Hu, J., Fu, R., and Cross, T.A. (2007). The chemical and dynamical influence of the anti-viral drug amantadine on the M2 proton channel transmembrane domain. Biophys. J. *93*, 276–283.

la Cour Jansen, T., Dijkstra, A.G., Watson, T.M., Hirst, J.D., and Knoester, J. (2006). Modeling the amide I bands of small peptides. J. Chem. Phys. *125*, 44312.

Law, R.J., Henchman, R.H., and McCammon, J.A. (2005). A gating mechanism proposed from a simulation of a human alpha7 nicotinic acetylcholine receptor. Proc. Natl. Acad. Sci. U.S.A. *102*, 6813–6818.

Li, C., Qin, H., Gao, F.P., and Cross, T.A. (2007). Solid-state NMR characterization of conformational plasticity within the transmembrane domain of the influenza A M2 proton channel. Biochim. Biophys. Acta *1768*, 3162–3170.

Lin, Y.-S., Shorb, J.M., Mukherjee, P., Zanni, M.T., and Skinner, J.L. (2009). Empirical amide I vibrational frequency map: application to 2D-IR line shapes from isotope-edited membrane peptide bundles. J. Phys. Chem. B. *113*, 592–602.

Manor, J., Khattari, Z., Salditt, T., and Arkin, I.T. (2005). Disorder influence on linear dichroism analyses of smectic phases. Biophys. J. *89*, 563–571.

Miyazawa, A., Fujiyoshi, Y., and Unwin, N. (2003). Structure and gating mechanism of the acetylcholine receptor pore. Nature *423*, 949–955.

Mukherjee, P., Krummel, A.T., Fulmer, E.C., Kass, I., Arkin, I.T., and Zanni, M.T. (2004). Site-specific vibrational dynamics of the CD3zeta membrane peptide using heterodyned two-dimensional infrared photon echo spectroscopy. J. Chem. Phys. *120*, 10215–10224.

Mukherjee, P., Kass, I., Arkin, I.T., and Zanni, M.T. (2006a). Structural disorder of the CD3zeta transmembrane domain studied with 2D IR spectroscopy and molecular dynamics simulations. J. Phys. Chem. B *110*, 24740–24749.

Mukherjee, P., Kass, I., Arkin, I.T., and Zanni, M.T. (2006b). Picosecond dynamics of a membrane protein revealed by 2D IR. Proc. Natl. Acad. Sci. U.S.A. *103*, 3528–3533.

Nishimura, K., Kim, S., Zhang, L., and Cross, T.A. (2002). The closed state of a H+ channel helical bundle combining precise orientational and distance restraints from solid state NMR. Biochemistry *41*, 13170–13177.

Pinto, L.H., Holsinger, L.J., and Lamb, R.A. (1992). Influenza virus M2 protein has ion channel activity. Cell *69*, 517–528.

Salom, D., Hill, B.R., Lear, J.D., and DeGrado, W.F. (2000). pH-dependent tetramerization and amantadine binding of the transmembrane helix of M2 from the influenza A virus. Biochemistry *39*, 14160–14170.

Sansom, M.S. (1995). Ion-channel gating. Twist to open. Curr. Biol. *5*, 373–375.

Schmidt, J.R., Corcelli, S.A., and Skinner, J.L. (2004). Ultrafast vibrational spectroscopy of water and aqueous N-methylacetamide: comparison comparison of different electronic structure/molecular dynamics approaches. J. Chem. Phys. *121*, 8887–8896.

Soskine, M., Mark, S., Tayer, N., Mizrachi, R., and Schuldiner, S. (2006). On parallel and antiparallel topology of a homodimeric multidrug transporter. J. Biol. Chem. *281*, 36205–36212.

Stouffer, A.L., Acharya, R., Salom, D., Levine, A.S., Di Costanzo, L., Soto, C.S., Tereshko, V., Nanda, V., Stayrook, S., and DeGrado, W.F. (2008). Structural basis for the function and inhibition of an influenza virus proton channel. Nature *451*, 596–599.

Tian, C., Gao, P.F., Pinto, L.H., Lamb, R.A., and Cross, T.A. (2003). Initial structural and dynamic characterization of the M2 protein transmembrane and amphipathic helices in lipid bilayers. Protein Sci. *12*, 2597–2605.

Torii, H., and Tasumi, M. (1992). Model-calculations on the amide-I infrared bands of globular-proteins. J. Chem. Phys. *96*, 3379–3387.

Torres, J., Adams, P.D., and Arkin, I.T. (2000a). Use of a new label, (13)==(18)O, in the determination of a structural model of phospholamban in a lipid bilayer. Spatial restraints resolve the ambiguity arising from interpretations of mutagenesis data. J. Mol. Biol. *300*, 677–685.

Torres, J., Kukol, A., and Arkin, I.T. (2000b). Use of a single glycine residue to determine the tilt and orientation of a transmembrane helix. A new structural label for infrared spectroscopy. Biophys. J. *79*, 3139–3143.

Torres, J., Kukol, A., Goodman, J.M., and Arkin, I.T. (2001). Site-specific examination of secondary structure and orientation determination in membrane proteins: the peptidic (13)C=(18)O group as a novel infrared probe. Biopolymers *59*, 396–401.

Wang, C., Lamb, R.A., and Pinto, L.H. (1995). Activation of the M2 ion channel of influenza virus: a role for the transmembrane domain histidine residue. Biophys. J. *69*, 1363–1371.

Zheng, J., Kwak, K., and Fayer, M.D. (2007). Ultrafast 2D IR vibrational echo spectroscopy. Acc. Chem. Res. *40*, 75–83.

Zhuang, W., Abramavicius, D., Hayashi, T., and Mukamel, S. (2006). Simulation protocols for coherent femtosecond vibrational spectra of peptides. J. Phys. Chem. B *110*, 3362–3374.

